

D , B and B_c exclusive weak decays

This chapter¹ contains a discussion of the different results obtained from the vertex sum rules for the weak semi-leptonic decays of the D , B and B_c . Intensive activities have been devoted to these processes during the last few years using different non-perturbative QCD approaches (QSSR [3,364,761–771]; light-cone sum rules [360,780–782]; lattice calculations [723]; heavy quark symmetry [164], and a perturbative factorization treatment within a heavy quark approach [784,600,601]). Here, we shall concentrate on the study of the previous decays from the point of view of QSSR from which we can extract the values of the form factors and some CKM mixing angles.

55.1 Heavy to light exclusive decays of the B and D mesons

55.1.1 Introduction and notations

One can extend the analysis carried out for the two-point correlator to the more complicated case of three-point function, in order to study the form factors related to the heavy to light transitions: $B \rightarrow K^* \gamma$ and $B \rightarrow \rho/\pi$ semi-leptonic decays. In contrast to the heavy to heavy transitions, where the symmetry of the heavy quarks can be exploited and which considerably simplifies the analysis, the heavy to light processes need non-perturbative approaches such as lattice or/and QSSR. For the QSSR approach, which we shall discuss here, we can consider the generic process:

$$B(D) \rightarrow L + \gamma(l\bar{\nu}), \quad (55.1)$$

and the corresponding three-point function:

$$V(p, p', q^2) \equiv - \int d^4x d^4y e^{i(p'x - py)} \langle 0 | T J_L(x) \mathcal{O}(0) J_B^\dagger(y) | 0 \rangle, \quad (55.2)$$

where J_L , J_B are the currents of the light and B mesons; \mathcal{O} is the weak operator specific for each process (penguin for the $K^* \gamma$, weak current for the semi-leptonic); $q \equiv p - p'$

¹ This is an extension and an update of the part of book [3] and the review given in [364].

and $q^2 \equiv t$.² The vertex obeys the double dispersion relation:

$$V(p^2, p'^2) \simeq \int_{M_b^2}^{\infty} \frac{ds}{s - p^2 - i\epsilon} \int_{m_l^2}^{\infty} \frac{ds'}{s' - p'^2 - i\epsilon} \frac{1}{\pi^2} \text{Im}V(s, s'). \quad (55.3)$$

As usual, the QCD part enters the LHS of the sum rule, while the experimental observables can be introduced through the spectral function after the introduction of the intermediate states:

$$V(p^2, p'^2) \simeq \frac{\langle 0|J_L(x)|L\rangle\langle L|\mathcal{O}(0)|B\rangle\langle B|J_B(y)|0\rangle}{(M_L^2 - p^2)(M_B^2 - p'^2)} + \text{higher states}. \quad (55.4)$$

M_L and M_B are respectively the masses of the final L and B mesons. The matrix elements are:

$$\langle 0|J_{P,B}(x)|P, B\rangle = \sqrt{2}f_{P,B}M_{P,B}^2, \quad \langle 0|J_V^\mu(x)|V\rangle = \frac{\sqrt{2}M_V^2}{2\gamma_V}\epsilon^\mu, \quad (55.5)$$

respectively, for pseudoscalar and vector states, where $f_\pi = 92.4$ MeV and $\gamma_\rho = 2.55$. The meson decay constants have been obtained either from the meson leptonic width or from the analysis of the two-point function discussed in the previous chapter of this book. Here, we shall be interested on the evaluation of the matrix element:

$$\langle L|\mathcal{O}(0)|B\rangle. \quad (55.6)$$

The improvement of the dispersion relation can be done in the way discussed previously for the two-point function. In the case of the heavy to light transition, where the two sum rule scales are quite different, the only possible improvement with a good M_b behaviour at large M_b (convergence of the QCD series³) is the so-called hybrid sum rule (HSR) corresponding to the uses of the moments for the heavy-quark channel and to the Laplace for the light one [721,761]:

$$\mathcal{H}(n, \tau') = \frac{1}{\pi^2} \int_{M_b^2}^{\infty} \frac{ds}{s^{n+1}} \int_0^{\infty} ds' e^{-\tau's'} \text{Im}V(s, s'). \quad (55.7)$$

Assuming that the higher state contributions to the spectral function are approximated by those of the QCD continuum from a threshold t_c and t'_c , and assuming that the QCD contribution also obeys a double dispersion relation, one obtains the FESR:

$$\mathcal{H}(n, \tau') = \frac{1}{\pi^2} \int_{M_b^2}^{t_c} \frac{ds}{s^{n+1}} \int_0^{t'_c} ds' e^{-\tau's'} \text{Im}V(s, s'). \quad (55.8)$$

² It has to be noticed that we shall use here, like in [761–764], the pseudoscalar current $J_P = (m_u + m_d)\bar{u}(i\gamma^5)d$ for describing the pion, where the QCD expression of the form factor can be deduced from the one in [767] by taking $m_c = 0$ and by remarking that the additional effect due to the light quark condensate for $B \rightarrow \pi$ relative to $B \rightarrow D$ vanishes in the sum rule analysis. In the literature [768,771], the axial-vector current has been used. However, as it is already well known in the case of the two-point correlator of the axial-vector current, by keeping its $q_\mu q_\nu$ part, (which is similarly done in the case of the three-point function) one obtains the contribution from the π plus the A_1 mesons but *not* the π contribution alone. Although, the A_1 effect can be numerically small in the sum rule analysis due to its higher mass, the mass behaviour of the form factor obtained in this way differs significantly from the one where the pseudoscalar current has been used due to the different QCD expressions of the form factor in the two cases.

³ One should notice here that contrary to the case of the double exponential (Borel) sum rule where the mixed condensate explodes, the OPE behaves quite well, at least to leading order in α_s .

Finally, in order to minimize the effects of the sum rule parameters into the analysis, it is usual to introduce the two-point sum rule expression of the decay constants and use a suitable relation between the three-point and two-point sum rules variables. These relations are [773] (obvious index notations):

$$\tau_3 = \frac{\tau_2}{2} \tag{55.9}$$

for the double Laplace sum rule (DLSR), and [763]:

$$n_3 = \frac{1}{2} \left(n_2 - \frac{1}{2} \right), \tag{55.10}$$

for the hybrid sum rule (HSR) and lead to a cancellation of the τ or n dependences in the sum rule analysis [768,731,761–766]. The different form factors entering the previous semi-leptonic and radiative processes are defined as:

$$\begin{aligned} \langle \rho(p') | \bar{u} \gamma_\mu (1 - \gamma_5) b | B(p) \rangle &= (M_B + M_\rho) A_1 \epsilon_\mu^* - \frac{A_2}{M_B + M_\rho} \epsilon^* p'(p + p')_\mu \\ &+ \frac{2V}{M_B + M_\rho} \epsilon_{\mu\nu\rho\sigma} p^\rho p'^\sigma, \\ \langle \pi(p') | \bar{u} \gamma_\mu b | B(p) \rangle &= f_+(p + p')_\mu + f_-(p - p')_\mu, \end{aligned} \tag{55.11}$$

and:

$$\begin{aligned} \langle K^*(p') | \bar{s} \sigma_{\mu\nu} \left(\frac{1 + \gamma_5}{2} \right) q^\nu b | B(p) \rangle &= i \epsilon_{\mu\nu\rho\sigma} \epsilon^{*\nu} p^\rho p'^\sigma F_1^{B \rightarrow K^*} \\ &+ \left\{ \epsilon_\mu^* (M_B^2 - M_\rho^2) - \epsilon^* q(p + p')_\mu \right\} \frac{F_1^{B \rightarrow K^*}}{2}. \end{aligned} \tag{55.12}$$

For completeness, we give the relations of these form factors to the decay rates of the B meson. In the case of the pseudoscalar final state, we have:

$$\frac{d\Gamma_+}{dt} = \frac{G_F^2 |V_{bq}|^2}{192\pi^3 M_B^3} \lambda^{3/2}(M_B^2, M_L^2, t) F_+^2(t), \tag{55.13}$$

while for the vector final state:

$$\begin{aligned} \frac{d\Gamma_+}{dt} &= \frac{G_F^2 |V_{bq}|^2}{192\pi^3 M_B^3} \langle^{1/2}(M_B^2, M_L^2, t) \\ &\times \left[2(F_0^A)^2 + \langle F_V^2 + \frac{1}{4M_F^2} ((M_B^2 - M_L^2 - t) F_0^A + \langle F_+^A \rangle)^2 \right], \\ \lambda &= \lambda(M_B^2, M_L^2, t). \end{aligned} \tag{55.14}$$

We have introduced the notation (often used in the literature):

$$\begin{aligned} F_+ &= f_+ & ; F_0^A &= (M_B + M_L)A_1; \\ F_+^A &= \frac{-A_2}{M_B + M_L}; F_V &= 0 \frac{V}{M_B + M_L}. \end{aligned} \quad (55.15)$$

55.1.2 Estimate of the form factors and of V_{ub}

In the numerical analysis, we obtain at $q^2 = 0$, the value of the $B \rightarrow K^* \gamma$ form factor [762]:

$$F_1^{B \rightarrow \rho} \simeq 0.27 \pm 0.03, \quad \frac{F_1^{B \rightarrow K^*}}{F_1^{B \rightarrow \rho}} \simeq 1.14 \pm 0.02, \quad (55.16)$$

which leads to the branching ratio $(4.5 \pm 1.1) \times 10^{-5}$, in perfect agreement with the CLEO data [16] $Br(B_0 \rightarrow K^{*0} \gamma) = (4.55 \pm 0.7 \pm 0.34) \times 10^{-5}$, and with the estimate in [781,820] and in [723]. for the D meson, one obtains:

$$F_1^{D \rightarrow \rho} \simeq 0.62 \pm 0.10, \quad \frac{F_1^{D \rightarrow K^*}}{F_1^{D \rightarrow \rho}} \simeq 1.22 \pm 0.04. \quad (55.17)$$

One should also notice that, in this case, the coefficient of the $1/M_b^2$ correction is very large, which makes the extrapolation of the c -quark results to higher values of the quark mass dangerous. This extrapolation is often done in some lattice calculations.

For the semi-leptonic decays $B \rightarrow \rho, \pi + l\nu$, QSSR gives a good determination of the ratios of the form factors with the values for the B-decays [763]:

$$\frac{A_2(0)}{A_1(0)} \simeq \frac{V(0)}{A_1(0)} \simeq 1.11 \pm 0.01, \quad \frac{A_1(0)}{F_1^{B \rightarrow \rho}(0)} \simeq 1.18 \pm 0.06, \quad \frac{A_1(0)}{f_+(0)} \simeq 1.40 \pm 0.06, \quad (55.18)$$

although their absolute values are quite inaccurate [761] and [771]. The direct determinations of the absolute values are given in Table 55.1, showing that different results are consistent with each others. The precise measurement of the ratios is due to the cancellation of systematic errors.

Combining these results with the ‘world average’ value of $f_+(0) = 0.25 \pm 0.02$ and the one of $F_1^{B \rightarrow \rho}(0)$, one can deduce the rates:

$$\Gamma_\pi \simeq (4.3 \pm 0.7) |V_{ub}|^2 \times 10^{12} \text{ s}^{-1}, \quad \Gamma_\rho / \Gamma_\pi \simeq 0.9 \pm 0.2. \quad (55.19)$$

These results indicate:

- The possibility to reach V_{ub} with a good accuracy from the exclusive modes. Using the accurate B lifetime $\tau_{B^+} = (1.655 \pm 0.027) \times 10^{-12} \text{ s}$, and the measured branching ratio into π [16], one can deduce:

$$V_{ub} = (3.6 \pm 0.3) \times 10^{-3}, \quad (55.20)$$

inside the range $(2 - 5) \times 10^{-3}$ given by PDG.

Table 55.1. Values of the different form factors in the D , B semi-leptonic processes at zero momentum from hybrid (HSR), double Laplace (DLSR)* and light cone (LCSR) sum rules

Process	$f_+(0)$	$A_1(0)$	$A_2(0)$	$V(0)$	Ref.
$D^0 \rightarrow \pi^- l \bar{\nu}$	0.7 ± 0.2				[769]
	0.5 ± 0.2				[771]
	0.65 ± 0.10				[772]
	$0.80^{+0.21}_{-0.14}$				[16] Data
$D^0 \rightarrow K^- l \bar{\nu}$	0.8 ± 0.2				[769]
	0.6 ± 0.13				[773]
	0.75 ± 0.12				[772]
	0.6 ± 0.1				[775]
	0.76 ± 0.03				[16] Data
$D^+ \rightarrow \text{scalar}$ $(\bar{u}u, \bar{s}d) l \bar{\nu}$	$0.42 - 0.57$				[776]
$D_s^+ \rightarrow \eta l \bar{\nu}$	0.50 ± 0.15				[777]
$D^0 \rightarrow \rho^- l \bar{\nu}$		0.5 ± 0.2	0.4 ± 0.1	1.0 ± 0.2	[771]
		0.34 ± 0.08	0.57 ± 0.08	0.98 ± 0.11	[772]
$D^0 \rightarrow K^{*-} l \bar{\nu}$		0.50 ± 0.15	0.60 ± 0.15	1.1 ± 0.25	[773]
		0.54 ± 0.04	0.67 ± 0.08	1.1 ± 0.1	[772]
		0.58 ± 0.03	0.41 ± 0.06	1.06 ± 0.09	[16] Data
$\bar{B}^0 \rightarrow \pi^+ l \bar{\nu}$	0.23 ± 0.02				[761] (DLSR + HSR)
	0.26 ± 0.02				[771]
	0.24 ± 0.03				[774]
	0.29 ± 0.04				[772]
	$0.24 - 0.29$				[778] (LCSR)
$\bar{B}^0 \rightarrow D l \bar{\nu}$	1.0 ± 0.2				[767]
	0.62 ± 0.06				[761]
$\bar{B}^0 \rightarrow \rho^+ l \bar{\nu}$		0.35 ± 0.16	0.42 ± 0.12	0.47 ± 0.14	[761] (DLSR + HSR)
		0.5 ± 0.1	0.4 ± 0.2	0.6 ± 0.2	[771]
$\bar{B}^0 \rightarrow K^{*+} \bar{\nu} \nu$		0.37 ± 0.03	0.40 ± 0.03	0.47 ± 0.03	[779]
$\bar{B}^0 \rightarrow D^* l \bar{\nu}$		0.46 ± 0.02	0.53 ± 0.09	0.58 ± 0.03	[761] (DLSR + HSR)

* If not mentioned DLSR have been used.

- One should also notice that the ratio between the widths into ρ and into π is about 1 due to the non-pole behaviour of A_1^B , while in different pole models, it ranges from 3 to 10. This result is in agreement within 1σ with the data (1.5 ± 0.5). Data on $B \rightarrow K(K^*) + \psi(\psi')$ decays [785] also favour this non-pole behaviour, while LCSR and lattice calculations indicate a slight increase of A_1 for increasing q^2 . However, the arguments given in [782] for explaining the failure of the standard QSSR approach is unclear to us and should deserve a further investigation. In the case

of the non-pole behaviour, one obtains a large negative value of the asymmetry α , contrary to the case of the pole models.

55.1.3 $SU(3)_F$ breaking in $\bar{B}/D \rightarrow Kl\bar{\nu}$ and determination of V_{cd}/V_{cs} and V_{cs}

We extend the previous analysis for the estimate of the $SU(3)_F$ breaking in the ratio of the form factors:

$$R_P \equiv f_+^{P \rightarrow K}(0)/f_+^{P \rightarrow \pi}(0), \quad (55.21)$$

where $P \equiv \bar{B}, D$. As mentioned before, we use the hybrid moments for the B and the double exponential sum rules for the D . The analytic expression of R_P is given in [764], which leads to the numerical result:

$$R_B = 1.007 \pm 0.020, \quad R_D = 1.102 \pm 0.007, \quad (55.22)$$

where one should notice that for $M_b \rightarrow \infty$, the $SU(3)$ breaking vanishes, while its size at finite mass is typically of the same sign and magnitude as the one of f_{D_s} or of the $B \rightarrow K^* \gamma$ discussed before. The previous value of R_D can be used with the data [16]:

$$\frac{Br(D^+ \rightarrow \pi^0 l \nu)}{Br(D^+ \rightarrow \bar{K}^0 l \nu)} = (8.5 \pm 3.4)\%, \quad (55.23)$$

for deducing the value of $|V_{cd}|/|V_{cs}|$

We can also determine directly from QSSR the absolute value of the $D \rightarrow K$ form factor. We obtain [764]:

$$f_+^{D \rightarrow K}(0) \simeq 0.80 \pm 0.16. \quad (55.24)$$

The data from D lifetime and De_3 [16] gives:

$$|f_+^{D \rightarrow K}(0)|^2 |V_{cs}|^2 \simeq 0.531 \pm 0.027. \quad (55.25)$$

Using the previous prediction for $f_+^{D \rightarrow K}(0)$ leads to:

$$V_{cs} = 0.91 \pm 0.18, \quad (55.26)$$

which differs slightly from the PDG prediction as the value of the form factor used there was 0.7 ± 0.1 . It is also expected that the most reliable result is the lower bound derived from Eq. (55.25) and from $f_+^{D \rightarrow K}(0) \leq 1$, which is:

$$V_{cs} \geq 0.73. \quad (55.27)$$

55.1.4 Large M_b -limit of the form factors

We have studied analytically the large M_b limit of some of the previous form factors [762–764]. We found that, within the approximation at which we are working, and to leading order in M_b , they are dominated, for $M_b \rightarrow \infty$, by the effect of the light-quark condensate,

which dictates (to leading order) the M_b behaviour of the form factors to be typically of the form:

$$F(0) \sim \frac{\langle \bar{d}d \rangle}{f_B} \left\{ 1 + \frac{\mathcal{I}_F}{M_b^2} \right\}, \quad (55.28)$$

where \mathcal{I}_F is the integral from the perturbative triangle graph, which is constant as $t_c'^2 E_c / \langle \bar{d}d \rangle$ (t_c' and E_c are the continuum thresholds of the light and b quarks) for large values of M_b . It indicates that at $q^2 = 0$ and to leading order in $1/M_b$, all form factors behave like $\sqrt{M_b}$, although, in most cases, the coefficient of the $1/M_b^2$ term is large, which explains the numerical dominance of the perturbative contribution at finite M_b . It should be finally noticed that owing to the overall $1/f_B$ factor, all form factors for the heavy to light transitions have a large $1/M_b$ correction.

55.1.5 q^2 -behaviour of the form factors

Although the sum rules give a reliable prediction for the value of the form factors at zero momentum transfer, the analysis of their q^2 behaviour is more delicate due to the eventual presence of non-Landau singularities [774] above a critical value:

$$t_{cr} = (M_Q + m_{q_2})^2, \quad (55.29)$$

for a $\bar{Q}q_1$ meson decaying semi-leptonically into a \bar{q}_1q_2 meson, where the weak current is $\bar{q}_2\gamma_\mu q_1$; M_Q and m_q are constituent quark masses. Much below t_{cr} , the sum rule result is expected to provide the right q^2 -behaviour of the form factor. The study of the q^2 behaviours of the B semi-leptonic form factors shows that, with the exception of the A_1 form factor, their q^2 dependence is only due to the non-leading (in $1/M_b$) perturbative graph, so that for $M_b \rightarrow \infty$, these form factors remain almost constant from $q^2 = 0$ to q_{\max}^2 , with a cautious for the accuracy of the result at q_{\max}^2 . The resulting M_b behaviour at q_{\max}^2 is the one expected from the heavy quark symmetry. The numerical effect of this q^2 -dependence at finite values of M_b is a polynomial in q^2 (which can be resummed), and mimics the pole parametrization quite well for a pole mass of about 6–7 GeV. The situation for the A_1 is drastically different from the other ones, as here the Wilson coefficient of the $\langle \bar{d}d \rangle$ condensate contains a q^2 dependence with a *wrong* sign and reads [763]:

$$A_1(q^2) \sim \frac{\langle \bar{d}d \rangle}{f_B} \left\{ 1 - \frac{q^2}{M_b^2} \right\}, \quad (55.30)$$

which, for $q_{\max}^2 \equiv (M_B - M_\rho)^2$, gives the expected behaviour:

$$A_1(q_{\max}^2) \sim \frac{1}{\sqrt{M_b}}. \quad (55.31)$$

One can notice that the q^2 dependence of A_1 is in complete contradiction with the pole behaviour due to its wrong sign. This result may explain the numerical analysis of [771].

One should notice that a recent phenomenological analysis of the data [783] on the large longitudinal polarization observed in $B \rightarrow K^* + \psi$ and a relatively small ratio of the rates $B \rightarrow K^* + \psi$ over $B \rightarrow K + \psi$ [785] can only be simultaneously explained if the $A_1(q^2)$ form factor decreases as indicated by our previous result, while larger choices of increasing or/and monotonically form factors fail to explain the data [786]. It is important to test this *anomalous* feature of the A_1 -form factor from some other data. One should notice that the q^2 behaviour of A_1 has also been studied from lattice calculations [723] and light-cone sum rule (LCSR) [780,782]. The latter result shows a slower increase of A_1 for increasing q^2 . Contrary to the interpretation given in [782] where the arguments given there are not clear to us (in particular the connection between the LCSR and the SVZ sum rule), the increase of the form factor may indicate that non-leading contributions at finite M_b , not accounted for in our approximation, can be numerically important, and competes with the leading-order contribution presented here. We plan to come back to this point in the near future. Finally, as a complement of the heavy quark symmetry which will be discussed in the next section, we have also presented in Table 55.1 the results for the $B \rightarrow D$, $D^* l \bar{\nu}$ form factors.

55.2 Slope of the Isgur–Wise function and value of V_{cb}

Using heavy quark symmetry in the infinite quark mass limit, the different form factors of the semi-leptonic $B \rightarrow D^*$ and $B \rightarrow D$ can be related to each others and expressed in terms of a single form factor:

$$f_+(q^2) = V(q^2) = A_0(q^2) = A_2(q^2) = \left(1 - \frac{q^2}{(M_B + M_D)^2}\right)^{-1} A_1(q^2), \quad (55.32)$$

where:

$$A_1(q^2) = \frac{M_B + M_D}{2\sqrt{M_B M_D}} \zeta(y). \quad (55.33)$$

$\zeta(y \equiv v \cdot v')$ is the so-called Isgur–Wise (IW) function and contains all non-perturbative QCD effects (v and v' are respectively the B and D meson velocity). At zero recoil $y = 1$, or at q_{\max}^2 , it is normalized as $\zeta(1) = 1$ from the conservation of the vector current. In this limit, the $B \rightarrow D^*$ decay distribution can be written as:

$$\begin{aligned} \frac{d\Gamma}{dy} &= \frac{G_F^2}{48\pi^3} (M_B - M_{D^*})^2 M_{D^*}^3 \sqrt{y^2 - 1} (y + 1)^2 \\ &\times \left[1 + \frac{4y}{y + 1} \frac{M_B^2 - 2y M_B M_{D^*} + M_{D^*}^2}{(M_B - M_{D^*})^2} \right] |V_{cb}|^2 \mathcal{F}^2(y), \end{aligned} \quad (55.34)$$

where $\mathcal{F}(y)$ is the IW function including perturbative and power corrections. Near zero

recoil, one can write the expansion:

$$\mathcal{F}(1) = \eta_A \left[1 + \frac{C_2}{M_Q^2} + \dots \right], \quad (55.35)$$

where η_A includes the perturbative corrections, which to two-loop accuracy reads [580]:

$$\eta_a = 0.960 \pm 0.007, \quad (55.36)$$

while, there is no $1/M$ correction in virtue of the Luke's theorem [568]. There are some attempts to estimate the size of the $1/M^2$ terms in the literature [164,562,587], which remain not under good control. The resulting compromise value is:

$$\mathcal{F}(1) \simeq 0.91(6), \quad (55.37)$$

where we have multiplied the quoted error by a factor 2 in order to be more conservative. Let me now discuss the slope of the IW function. De Rafael and Taron [789] have exploited the analyticity of the elastic b -number form factor F defined as:

$$\langle B(p') | \bar{b} \gamma^\mu b | B(p) \rangle = (p + p')^\mu F(q^2), \quad (55.38)$$

which is normalized as $F(0) = 1$ in the large mass limit $M_B \simeq M_D$. Using the positivity of the vector spectral function and a mapping in order to get a bound on the slope of F outside the physical cut, they obtained a rigorous though weak bound:

$$F'(vv' = 1) \geq -6. \quad (55.39)$$

Including the effects of the Υ states below $\bar{B}B$ thresholds by assuming that the $\Upsilon \bar{B}B$ couplings are of the order of 1, the bound becomes stronger:

$$F'(vv' = 1) \geq -1.5. \quad (55.40)$$

Using QSSR, we can estimate the part of these couplings entering in the elastic form factor. We obtain the value of their sum [765]:

$$\sum g_{\Upsilon \bar{B}B} \simeq 0.34 \pm 0.02. \quad (55.41)$$

In order to be conservative, we have multiplied the previous estimate by a factor 3 larger. We thus obtain the improved bound:

$$F'(vv' = 1) \geq -1.34, \quad (55.42)$$

but the gain over the previous one is not much. Using the relation of the form factor with the slope of the IW function, which differs by $-16/75 \log \alpha_s(M_b)$ [790], one can deduce the final bound [765]:⁴

$$\zeta'(1) \geq -1.04. \quad (55.43)$$

⁴ Voloshin in [791] derives also the upper bound $\rho^2 \leq 1/4 + \bar{\Lambda}/[2(M_{B'} - M_B)]$, which, however, depends crucially on the less controlled value of $\bar{\Lambda}$ and the mass of the radial excitation $M_{B'}$.

The previous bound combined with the Bjorken lower bound [792] leads to the allowed domain:

$$\frac{1}{4} \leq \rho^2 \equiv -\zeta'(1) \leq 1.04. \quad (55.44)$$

However, one can also use the QSSR expression of the IW function from vertex sum rules [655] in order to extract the slope *analytically*. To leading order in $1/M$, the *physical* IW function reads [Rep. 18.5]:

$$\zeta_{\text{phys}}(y \equiv vv') = \left(\frac{2}{1+y} \right)^2 \left\{ 1 + \frac{\alpha_s}{\pi} f(y) - \langle \bar{d}d \rangle \tau^3 g(y) + \langle \alpha_s G^2 \rangle \tau^4 h(y) + g \langle \bar{d}Gd \rangle \tau^5 k(y) \right\}, \quad (55.45)$$

where τ is the Laplace sum rule variable and f , h and k are analytic functions of y . From this expression, one can derive the analytic form of the slope [765]:

$$\zeta'_{\text{phys}}(y=1) \simeq -1 + \delta_{\text{pert}} + \delta_{NP}, \quad (55.46)$$

where at the τ -stability region:

$$\delta_{\text{pert}} \simeq -\delta_{NP} \simeq -0.04, \quad (55.47)$$

which shows the near-cancellation of the non-leading non-perturbative corrections at this *leading order in $1/M$* . Adding a generous 50% error of 0.02 for the correction terms, we finally deduce the *leading order result in $1/M$* :

$$\zeta'_{\text{phys}}(y=1) \simeq -1 \pm 0.02. \quad (55.48)$$

Using this result in different existing model parametrizations, we deduce the value of the mixing angle, *to leading order in $1/M$* :

$$V_{cb} \simeq \left(\frac{1.48 \text{ ps}}{\tau_b} \right)^{1/2} \times (37.3 \pm 1.2 \pm 1.4) \times 10^{-3}, \quad (55.49)$$

where the first error comes from the data and the second one from the model-dependence.⁵

In order to discuss the effects due to the $1/M$ corrections, we proceed in the following phenomenological way:

- We use the predicted value of the form factor 0.91 ± 0.03 at $y=1$,
- We also use the value 0.53 ± 0.09 at $q^2=0$ [761]⁶ from the sum rule in the full theory (i.e without using a $1/M$ -expansion).
- We join the two results, where the model dependence of the analysis enters through the concavity of the form factor between these two extreme boundaries.

⁵ A recent analysis [574] relates the curvature with the slope, such that in this case, the model dependence of the result disappears.

⁶ This value is just on top of the CLEO data [793].

Table 55.2. Different QSSR estimates of the slope of the IW-function compared with the lattice result

$-\zeta' \equiv \rho^2$	References	Comments
0.84 ± 0.02	[795]	Numerical fit
0.70 ± 0.1	[796]	
0.70 ± 0.25	[797]	
1.00 ± 0.02	[765]	Analytic expression
0.91 ± 0.04		QSSR average
$(0.9_{-0.3}^{+0.2} \text{ }_{-0.4}^{+0.4})$	[798]	Lattice

If we use the value of the concavity given by [574], the form factor can be parametrized as:

$$F(y) = F(1)\{1 + \hat{\zeta}'(y - 1) + \hat{c}(y - 1)^2\}, \quad (55.50)$$

where:

$$\hat{\zeta}' = \zeta' - (0.16 \pm 0.02), \quad \hat{c} \approx -0.66\hat{\zeta}' - 0.11. \quad (55.51)$$

Therefore, we can deduce the slope:

$$\zeta' \simeq -(0.75 \pm 0.1), \quad (55.52)$$

which can indicate that the $1/M$ correction also tends to decrease the value of $|\zeta'|$. This leads to the *final* estimate:

$$V_{cb} \simeq \left(\frac{1.48 \text{ ps}}{\tau_b}\right)^{1/2} \times (38.8 \pm 1.2 \pm 1.5 \pm 1.5) \times 10^{-3}, \quad (55.53)$$

where the new last error is induced by the error from the slope, while the model dependence only brings a relatively small error. Using the measured B^0 -lifetime $\tau_B = 1.548 \pm 0.032$ ps, one obtains:

$$V_{cb} \simeq (37.9 \pm 2.4) \times 10^{-3}, \quad (55.54)$$

compared with the value 0.0402 ± 0.0019 from LEP measurements of exclusive and inclusive decays [16] and CLEO data [793]. Our result for the slope is also in good agreement with the data. Finally, we compare the different results from the sum rules in Table 55.2, from which we deduce the *weighted average* from the sum rules given in Table 55.2, where we have taken the error of the most precise determinations which we have multiplied by a factor 2 in order to be conservative. This average is in good agreement with the lattice value, which is also given in this table.

55.3 $B^*(D^*) \rightarrow B(D) \pi(\gamma)$ couplings and decays

In [766], we have further applied the vertex sum rules in order to study the decays and couplings of the $B^*(D^*) \rightarrow B(D) \pi(\gamma)$, using systematically a $1/M_b$ expansion in the full theory. The couplings are defined as:

$$\begin{aligned} \langle B^*(p)B(p')\pi(q) \rangle &= g_{B^*B\pi} q_\mu \epsilon^\mu, \\ \langle B^*(p)B(p')\gamma(q) \rangle &= -e g_{B^*B\gamma} p_\alpha p'_\beta \epsilon^{\mu\nu\alpha\beta} \epsilon_\mu \epsilon'_\nu, \end{aligned} \quad (55.55)$$

where $q \equiv p' - p$ and $-Q^2 \equiv q^2 \leq 0$, while ϵ_μ are the polarization of the vector particles. Our numerical predictions for the couplings are:⁷

$$g_{B^*B\pi} \simeq 14 \pm 4, \quad g_{D^*D\pi} \simeq 6.3 \pm 1.9, \quad (55.56)$$

in good agreement with the results in [800] obtained by combining QSSR with soft pion techniques. These results lead to the prediction:

$$\Gamma_{D^{*-} \rightarrow D^0 \pi^-} \simeq 1.54 \Gamma_{D^{*0} \rightarrow D^0 \pi^0} \simeq (8 \pm 5) \text{ keV}, \quad (55.57)$$

where we have assumed an isospin invariance for the couplings.

We notice that in the large M_b limit, the perturbative graph gives the leading contribution like some other heavy-to-heavy processes studied within the same approach. In this limit, we obtain:

$$g_{B^*B\pi} \simeq \frac{2M_B}{\sqrt{2}f_\pi} g^\infty \left\{ 1 + \frac{E_c^B}{M_b} + \frac{\pi^2}{2} \frac{\langle \bar{u}u \rangle}{(E_c^B)^3} \right\}, \quad (55.58)$$

where g^∞ is the static coupling:

$$g^\infty \equiv \frac{N_C}{2} \left(\frac{m_u + m_d}{m_\pi^2} \right) (0.12 E_c^\infty) \simeq (0.15 \pm 0.03), \quad (55.59)$$

for $E_c^\infty \simeq (1.6 \pm 0.1) \text{ GeV}$.

In the same way, we have also estimated the $B^*B\gamma$ and $D^*D\gamma$ couplings. We obtain:

$$\Gamma_{B^{*-} \rightarrow B^- \gamma} \simeq 2.5 \Gamma_{B^{*0} \rightarrow B^0 \gamma} \simeq (0.10 \pm 0.03) \text{ keV}. \quad (55.60)$$

For the D^* meson, one obtains:

$$\Gamma_{D^{*0} \rightarrow D^0 \gamma} \simeq (7.3 \pm 2.7) \text{ keV}, \quad \Gamma_{D^{*-} \rightarrow D^- \gamma} \simeq (0.03 \pm 0.08) \text{ keV}, \quad (55.61)$$

which despite the large errors, shows in the analysis that the heavy quark contribution acts in the right direction for explaining the large charge dependence of the observed rates:

$$\Gamma_{D^{*0} \rightarrow D^0 \pi^0} / \Gamma_{D^{*0} \rightarrow D^0 \gamma}, \quad \Gamma_{D^{*-} \rightarrow D^0 \pi^-} / \Gamma_{D^{*-} \rightarrow D^- \gamma}. \quad (55.62)$$

⁷ The application of the $1/M$ expansion to the D and D^* mesons might be a very crude approximation. A comparison of the result with the recent CLEO data [799] $g_{D^*D\pi} = 17.9 \pm 0.3 \pm 1.9$ needs further investigation using a complete QCD expression of the vertex.

Table 55.3. Comparison of semi-leptonic form factors for different decays. We compare the dimensionless quantities f_+ , A_1 , A_2 , V related to F_0^A , F_+^A and F_V through Eq. (55.15)

Channels	Reference	f_+	V	A_2	A_1
$c\bar{c}$	[731]	0.55 ± 0.10	0.48 ± 0.07	0.30 ± 0.05	0.30 ± 0.05
	[801]	0.20 ± 0.01	0.37 ± 0.1	0.27 ± 0.03	0.28 ± 0.01
$b\bar{b}$	[731]	0.60 ± 0.12	1.6 ± 0.3	0.06 ± 0.06	0.40 ± 0.10
	[801]	0.30 ± 0.05	2.1 ± 0.25	0.39 ± 0.05	0.35 ± 0.20
$B \rightarrow D^{(*)}$	[771]	0.75 ± 0.05	0.8 ± 0.1	0.68 ± 0.08	0.65 ± 0.10
	[803]	0.69	0.71	0.69	0.65
	[48]	0.62 ± 0.06	0.58 ± 0.03	0.53 ± 0.09	0.46 ± 0.02
	$B_c \rightarrow \eta_c$	$B_c \rightarrow B_s$	$B_c \rightarrow B$	$B_c \rightarrow D$	
	$B_c \rightarrow J/\psi$	$B_c \rightarrow B_s^*$	$B_c \rightarrow B^*$	$B_c \rightarrow D^*$	
$F_+(0)$	0.55 ± 0.10	0.60 ± 0.12	0.48 ± 0.14	0.18 ± 0.08	
$F_V(0)$ [GeV $^{-1}$]	0.048 ± 0.007	0.15 ± 0.02	0.11 ± 0.02	0.02 ± 0.01	
$F_+^A(0)$ [GeV $^{-1}$]	-0.030 ± 0.003	-0.005 ± 0.005	0.005 ± 0.005	0.010 ± 0.010	
$F_0^A(0)$ [GeV]	3.0 ± 0.5	3.3 ± 0.7	1.7 ± 0.7	0.8 ± 0.4	

One should also notice that the non-leading $1/M_b$ corrections are large in the two channels. For the $PP^*\pi$ coupling, these corrections coming mainly from the perturbative graph tend to cancel, which imply the validity of the HQET result:

$$g_{B^*B\pi} f_{B^*} \sqrt{M_B} \simeq g_{D^*D\pi} f_{D^*} \sqrt{M_D}. \quad (55.63)$$

For the electromagnetic, these large corrections are necessary to explain the large charge dependence of the ratio of the $D^{*0} \rightarrow D^0\gamma$ over the $D^{*-} \rightarrow D^-\gamma$ observed widths. However, the new CLEO data give $\Gamma_{D^{*-} \rightarrow D^-\gamma} \simeq (96 \pm 22)$ keV indicating that the $1/M$ approach for the absolute width can be a bad approximation.

55.4 Weak semi-leptonic decays of the B_c mesons

The analysis of the semi-leptonic decays of the B_c meson has been performed in [731] using QSSR methods. The procedure is very similar to the one used in the previous sections. The principal results of the sum rules evaluation of the form factors in Eq (55.11) are collected in Table 55.3. The value with the lower (resp. larger) modulus corresponds to the value of the continuum energy $E_c = 1$ GeV (resp. 2 GeV). In Fig. 55.1, we show the q^2 behaviour of the $B_c \rightarrow \eta_c l \bar{\nu}$ process, which shows a net deviation of the QSSR prediction from the monopole fit:

$$F_+(t) = \frac{F_+(0)}{1 - t/M_{\text{pole}}^2}, \quad (55.64)$$

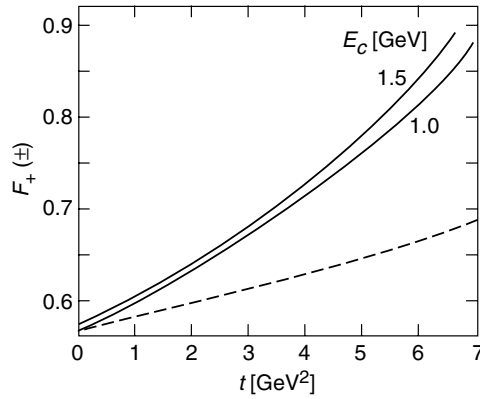


Fig. 55.1. q^2 behaviour of the $B_c \rightarrow \eta_c l \bar{\nu}$ form factor: QSSR predictions with polynomial fit (continuous line) for two values of E_c ; monopole parametrization with $M_{\text{pole}} = M_{B_c^*} = 6.33$ GeV.

with $M_{\text{pole}} = M_{B_c^*}$, which can be tested experimentally. The same feature is observed in other channels. For the $B_c \rightarrow J/\psi l \bar{\nu}$ process, one obtains the fitted QSSR pole mass:

$$F_V : M_{\text{pole}} \simeq 4.08 \text{ GeV}, \quad F_+^A : M_{\text{pole}} \simeq 4.44 \text{ GeV}, \quad F_0^A : M_{\text{pole}} \simeq 4.62 \text{ GeV}. \tag{55.65}$$

However, the question is, whether it is known if the previous q^2 -behaviour deviation from the monopole model is an artifact of sum rule or something more fundamental. In VDM, the vector current couples to the hadrons with appropriate flavour content, where the intermediate vector mesons leads to the pole of the form factor $F_+(t)$ at $t \equiv q^2 = M_V^2$ giving the t -behaviour in Eq. (55.64), while an intuitive quark model form factor determined by the Fourier transform of the hadron wave function gives:

$$F_+(t) = 1 + \frac{\langle r^2 \rangle}{6} t + \mathcal{O}(t^2), \tag{55.66}$$

where $\langle r^2 \rangle$ is the hadron mean-squared radius in the quark model. For light hadrons, the vector meson is the ρ meson. Expanding Eq. (55.64) in t , and identifying with Eq. (55.66), one obtains:

$$\sqrt{\langle r^2 \rangle}_\pi = \frac{\sqrt{6}}{M_\rho} \simeq 0.6 \text{ fm}, \tag{55.67}$$

which is a reasonable value for the quark model, while for the case of the B_c meson, the vector meson is the B_c^* with a mass of 6.4 GeV leading to a mean radius of about 0.08 fm, which is too small for a reliable validity of the non-relativistic quark model. This feature might indicate that the non-relativistic picture is not reasonable, such that, we have, instead, to discuss the problem within a relativistic field theory approach such as QSSR. We compare in Table 55.4 different theoretical predictions based on QCD-like models.

Table 55.4. *Partial decay rates for B_c and B_c^* mesons*

Channels	Reference	Rates in 10^{10}s^{-1}
$B_s l\nu$	[731]	0.35 ± 0.10
	[801]	0.18
$B_s^* l\nu$	[731]	0.35 ± 0.10
	[801]	0.87
$b\bar{s}l\nu$	[731]	
	[801]	
	[802]	2.91
$\eta_c l\nu$	[731]	0.27 ± 0.07
	[801]	0.03
$J/\psi l\nu$	[731]	0.32 ± 0.08
	[801]	0.21
$c\bar{c}l\nu$	[731]	
	[801]	
	[802]	6.90

55.4.1 Anomalous thresholds

Another subtle point in the vertex sum rule approach is the eventual existence of anomalous thresholds in the study of the q^2 behaviour of the form factors [804–806]. Let's illustrate the analysis from the study of the process $B_c(\bar{b}c) \rightarrow \Psi(\bar{c}c)l\bar{\nu}$. The interaction between \bar{b} and c leads to the formation of the vector meson $B_c^*(\bar{c}b)$ allowing us to approximate the singularity by the pole of the vector meson mass near the *normal threshold* $t_n = (M_b + M_c)^2$, where t should be large enough for ensuring the \bar{b} and c quark on-mass shell. *Anomalous threshold* occurs, if under a certain condition, for smaller value t_a of t , one is able to give on-shell mass b a gentle kick in order to transform it into an on-shell mass c . The derivation of the existence of anomalous thresholds can be simply done using dual diagrams [804] shown in Fig. 55.2. The dual (b) of the QCD three-point function (a) can be obtained by transforming the plane segments A , B , C , O of the planar diagram (a) into points of the dual diagram connected by lines with lengths given by the masses of the particles dividing the segments. If the point O of the dual diagram is inside the triangle ABC , then there exists an anomalous threshold and its value is given by the square of the distance AB . For the B_c of mass 6.25 GeV, anomalous thresholds do exist for the decay $B_c \rightarrow \eta_c$, J/Ψ provided the quark mass fulfill the conditions: $m_c < 2.1$ GeV and $m_b < 5.9$ GeV, which are satisfied by any quark models. The exact position of the anomalous threshold depends strongly on the value of the quark masses. Using the constituent (pole) masses $m_b = 4.9$ GeV and $m_c = 1.57$ GeV, one would obtain $\sqrt{t_a} = 4.6$ GeV, while the minimum possible value is $\sqrt{t_a} \geq m_b - m_c = 3.3$ GeV. These values are consistent with the effective pole mass of about 4.2 GeV found in the sum rule analysis. Everything looks consistent except

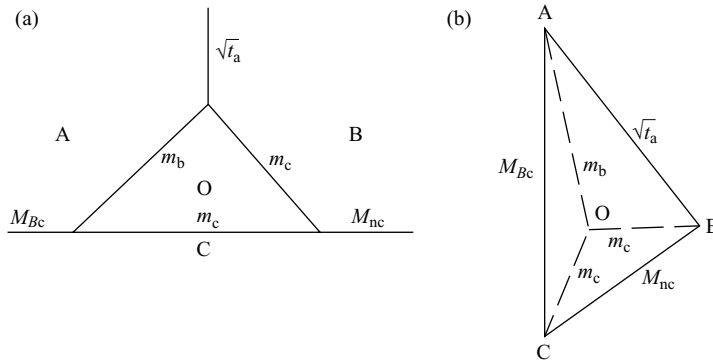


Fig. 55.2. QCD three-point function (a) and its dual diagram (b).

that quarks are not free particles while perturbation theory breaks down if one tries to approach the pole of the quark propagators. Therefore, an anomalous threshold should not be present in the t -dependence of the (hadronic) form factors. The same conclusion holds for the normal thresholds, as in the e^+e^- process, we do not observe a quark-antiquark state but hadrons. Quark-hadron duality tells us that the discontinuity across the quark-antiquark cut, if viewed from a certain distance or smeared over some energy interval describes the hadronic production in e^+e^- quite well. In a QCD-like model, [805,806] found that although quark anomalous thresholds are absent, at some distance from the calculated threshold, the amplitude can be quite well approximated by anomalous singularities at the quark level.